

3D Whole Hand Targets: Evaluating Slap and Contactless Fingerprint Readers

Sunpreet S. Arora¹, Anil K. Jain¹, and Nicholas G. Paulter Jr.²

Abstract: We design and fabricate wearable whole hand 3D targets complete with four fingerprints and one thumb print for evaluating multi-finger capture devices, e.g., contact-based and contactless slap readers. We project 2D calibration patterns onto 3D finger surfaces pertaining to each of the four fingers and the thumb to synthetically generate electronic 3D whole hand targets. A state-of-the-art 3D printer is then used to fabricate physical 3D hand targets with printing materials that are similar in hardness and elasticity to the human skin and are optically compatible for imaging with a variety of fingerprint readers. We demonstrate that the physical 3D whole hand targets can be imaged using three commercial (500/1000 ppi) *Appendix F* certified contact-based slap fingerprint readers and a *PIV* certified contactless slap reader. We further show that the features present in the 2D calibration patterns (e.g. ridge structure) are replicated with high fidelity on both the electronically generated and physically fabricated 3D hand targets. Results of evaluation experiments for the three contact-based slap readers and the contactless slap reader using the generated whole hand targets are also presented. This study, for the first time, demonstrates the utility of the 3D wearable hand targets for evaluation of slap readers, both contact and contactless.

Keywords: 3D whole hand targets, 3D printing, fingerprint reader evaluation, slap readers, contactless readers

1 Introduction

With a variety of fingerprint readers being commercially available for use in biometric applications, there is a growing interest amongst metrology agencies (e.g. the National Institute of Standards and Technology (NIST)) to design and develop standard artifacts and procedures for consistent and reliable evaluation of fingerprint readers. Existing fingerprint reader evaluation standards [Ni06] [Ni13] prescribe the use of 2D/3D targets for testing different aspects of a fingerprint reader, such as geometric accuracy, resolution and spatial frequency response [FB]. Fingerprint vendors often use standard 2D targets for this assessment. While useful for evaluating fingerprint readers, 2D targets are not adequate to simulate how users interact with the reader during the fingerprint capture process (e.g. finger/hand placement on the reader platen for contact-based capture or orienting finger/hand appropriately over the reader for contactless capture). To overcome this limitation, we designed and fabricated 3D targets with skin-like hardness and elasticity that could be worn on a finger to mimic the fingerprint capture process [Ar16]. We projected 2D calibration patterns of known characteristics (e.g. fingerprints with known ridge flow, ridge spacing and minutiae or sine gratings of pre-specified orientation and spacing) onto a 3D finger surface of known dimensions to create electronic 3D targets. The electronic 3D targets were fabricated using a state-of-the-art 3D printer (Stratasys Objet350 Connex³); the printed targets were then successfully used for evaluating single-finger optical readers.

¹ Department of Computer Science and Engineering, Michigan State University, East Lansing, MI, 48824. Email: {arorasun, jain}@cse.msu.edu

² National Institute of Standards and Technology, 100 Bureau Dr., Gaithersburg, MD, 20899. Email: paulter@nist.gov

³ The mention of companies and products here does not imply endorsement or recommendation of those companies or products by the authors or the organizations they represent.

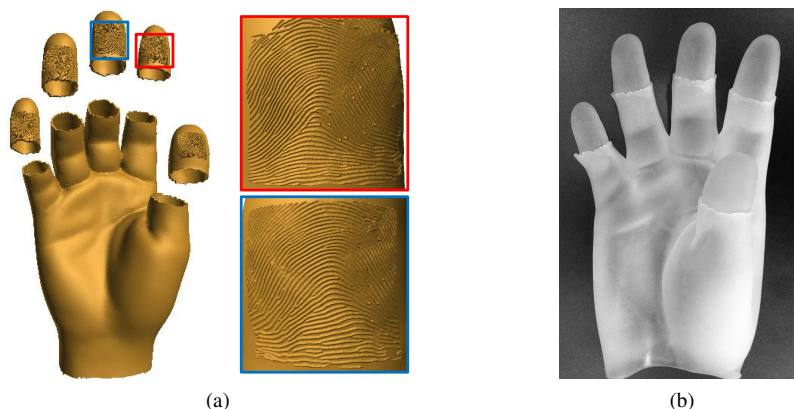


Fig. 1: 3D whole hand target for evaluating slap and contactless fingerprint readers. (a) Electronic 3D hand target complete with the four fingers, thumb and fingerless glove; the index and middle fingerprints engraved on the target are shown at full scale in red and blue boxes, respectively. (b) Fabricated hand target with translucent rubber-like material TangoPlus FLX930 [Stb].

Fingerprint recognition systems designed for large-scale applications (e.g. law enforcement [Ne12], homeland security [Of] and national ID programs [Aa]) generally require capturing all ten fingerprints (tenprints) of a person during enrolment. To maintain high throughput, tenprint acquisition is usually done by capturing two slap impressions⁴ of the four fingers of the left and right hand, followed by simultaneous capture of the two thumbprints (also termed as 4-4-2 capture) using a slap fingerprint reader. The quality of the acquired slap impression is a function of several user-dependent variables, e.g., the pressure applied on the reader platen by each finger, and the relative orientation of the fingers with respect to each other and the reader platen, as well as the reader optics.

Contact-based slap capture, however, induces distortion in the captured image due to flattening of the skin when the fingers are pressed against the reader platen. It is also typically required to clean the reader platen after every few captures to prevent accumulated residue due to repeated use of the reader from impacting the quality of the captured image. Further, some users have hygiene-related concerns in using contact-based readers. To alleviate these issues, contactless slap fingerprint capture technology was introduced, and has since garnered significant attention [PC09]. In 2007, the National Institute of Justice (NIJ) initiated the fast capture initiative to create new technology that will automatically “capture the same images as 10 rolled fingerprints in less than 15 seconds and both palm prints in less than 1 minute” [Fa]. The goal of NIJ’s initiative was to improve fingerprint image quality and the commercialization of contactless fingerprint readers for law enforcement and homeland security agencies. Given that almost all criminal fingerprint databases contain rolled prints, another objective of this initiative was to improve fingerprint identification accuracy by comparing rolled prints to rolled prints rather than slap to rolled prints. Since then, significant advances have been made in the design and development of commercial-grade contactless slap fingerprint readers.

An important requirement for acquiring good quality fingerprint images using contactless slap readers is the proper positioning of the user’s hand/finger with respect to the optical capture set-up of the reader. Given that user-induced variabilities can impact the quality of fingerprint images acquired by contactless slap readers, it is important to evaluate the readers to ensure that image quality suffices for fingerprint recognition, i.e., comparing acquired fin-

⁴ A four-finger simultaneous capture (index, middle, ring and little fingers altogether) is called a *slap impression*.



Fig. 2: Images of a 3D fingerprint target fabricated with translucent rubber-like material TangoPlus FLX930 [Stb] (shown in (a)) captured by three different *PIV* certified [Ni06] single-finger optical readers using different wavelengths of light for fingerprint capture: (b) blue wavelength, (c) combination of blue and red wavelengths, and (d) red wavelength. Targets printed with black colored rubber-like materials (TangoBlackPlus FLX980 [Stb] and FLX9840-DM [Sta]) could not be imaged using these three readers.

gerprint images to rolled (or slap) prints in the database. While evaluation procedures have been developed to assess contact-based fingerprint readers [Ni06] [Ni13], there is still an impending need to develop methods, metrics and artifacts for evaluation of contactless fingerprint readers. For this reason, NIST started the Contactless Fingerprint Capture Device Measurement Research Program with the aim of “developing methodologies for measuring the image fidelity of contactless fingerprint capture devices” [Co].

We have designed and fabricated whole hand targets (both electronic and physical) for evaluating contact-based and contactless slap fingerprint readers (see Fig. 1). To create a whole hand target, we first segment an electronic 3D hand surface⁵ into six different parts: four individual fingers, the thumb, and the remaining middle portion of the hand surface⁶. Individual targets for the four fingers and the thumb are created by projecting pre-specified 2D calibration patterns onto 3D finger surfaces using the method described in [Ar16]. The middle portion of the hand surface is synthetically processed to make a wearable fingerless glove. Each of the six parts of the whole hand are printed using a state-of-the-art 3D printer (Stratasys Objet350/500 Connex⁴⁷) with materials that are similar in hardness and elasticity to the human skin as well as appropriate for imaging with optical readers. The printer slices 3D parts into 2D horizontal layers and prints them layer by layer. It uses a support material to prevent the parts being printed from breaking. The bulk of the support material can be manually removed from the printed parts. However, to remove any support material debris remaining on the printed parts, the individual parts are subsequently cleaned with 2M NaOH solution and water. The printed parts are then physically assembled to create the whole hand target (see Fig. 1(b)).

The printed 3D hand targets can be imaged using three different commercial (500/1000 ppi) *Appendix F* certified contact-based slap fingerprint readers and a *PIV* certified contactless

⁵ 3D hand surface can either be obtained directly using a 3D scanner or synthetically generated. We use a synthetically designed 3D hand surface.

⁶ A single 3D hand target model with all five fingerprints becomes quite complex due to the resolution requirements for engraving fingerprints. Because the 3D printer software does not accept large electronic model files (>100 MB), the hand target is designed and manufactured in parts.

⁷ The two printers have X and Y resolution of 600 dpi and Z resolution of 1600 dpi. This suffices for printing targets with micron-scale gratings, e.g., fingerprints.

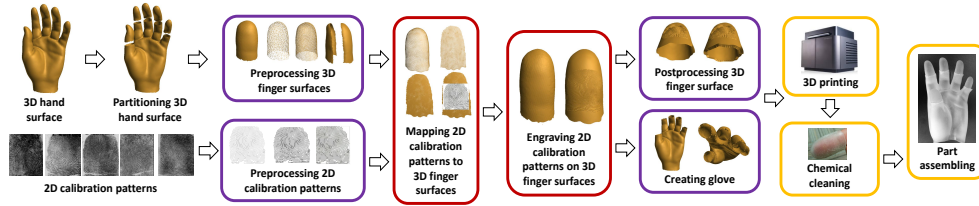


Fig. 3: Generating a 3D whole hand target from a generic 3D hand surface and a set of 2D calibration patterns.

slap reader⁸. We extract individual plain prints⁹ for each finger from slap impressions of the whole hand targets captured using the three slap readers and show that they can be successfully matched to (i) the original 2D fingerprints used to create the whole hand target, and (ii) the frontal images of electronic whole hand targets. We also conduct experiments to evaluate the three slap readers and the contactless slap reader using the generated whole hand target. The contributions of our research are as follows:

1. Generation of whole hand target for evaluating contact-based and contactless slap fingerprint readers. In our earlier work [Ar16], we had generated individual finger targets for evaluating single-finger contact-based optical readers only. We further extend our method to generate a whole hand target for use with multi-finger optical devices, e.g. slap fingerprint readers.
2. Use of optically compatible 3D printing materials for fabricating 3D targets. In our earlier work [Ar16], we had printed 3D targets with materials similar in hardness and elasticity to the finger skin (TangoBlackPlus FLX980 [Stb] and FLX9840-DM [Sta]⁴). However, these materials were black in color, and could not be imaged with optical readers using certain light wavelengths (e.g. blue). To remedy this, we now use translucent whitish rubbery materials (TangoPlus FLX930 [Stb] and FLX9740-DM [Sta]⁴) that provide the desired hardness and elasticity as well as appropriate optical properties for use with a variety of contact-based optical fingerprint readers (see Fig. 2). A bluish-gray colored rigid opaque material (RGD8520-DM [Sta]) is used to manufacture fingerprint targets for the contactless slap reader. This material provides optimum contrast between fingerprint ridges and valleys for imaging the target with the contactless slap reader.

2 Generating Whole Hand Target

Let a generic electronic 3D hand surface be denoted by H . Assume that the electronic surface H is a triangular mesh with a set of vertices V_H and a set of triangles T_H . Each vertex, v , in V_H has (x, y, z) coordinates corresponding to its spatial location in H , and each triangle in T_H connects a unique set of three vertices in V_H . As mentioned earlier, the whole hand target W is generated from H in parts. Assume that the 2D calibration pattern to be projected onto the i^{th} finger in H is denoted by I_i ($i = \{1 \dots 5\}$). The complete process to create the whole hand target W , given H and the set of 2D calibration patterns I , is described below (see Fig. 3, adapted from [Ar16]).

⁸ The contactless slap reader captures four fingerprints (index, middle, ring and little fingers) with a single hand movement.

⁹ The term *plain print* is used to refer to the fingerprint impression of an individual finger extracted from the slap impression [Re].

1. **Partitioning 3D hand surface:** The electronic hand surface H is divided into six different parts: the four fingers S_i ($i=\{1..4\}$), the thumb S_5 , and the remaining middle portion M of the hand surface, which can be described as a *fingerless glove*. The selector tool in open-source 3D mesh processing software Meshlab [Me] is used for selecting the different parts. A new mesh layer is then created for each selected part. The registration of the six parts with respect to each other remains intact while partitioning the hand surface. This facilitates assembly of the fabricated parts to create the whole hand target. Assume that the set of vertices and triangles present in each 3D finger surface S_i is denoted by V_i and T_i , respectively. Also, let $I_i(u, v)$ denote the grayscale value at spatial coordinates (u, v) in the calibration pattern I_i .
2. **Preprocessing 3D finger surfaces:** Electronic finger surface S_i is aligned such that the finger length is along the y-axis in S_i . The surface S_i is re-meshed by sampling vertices from the set V_i based on the curvature of S_i [PC06]. Surface re-meshing reduces the density of S_i , therefore, S_i is subdivided using Loop's method [Lo87] to ensure sufficient fidelity during projection of the 2D calibration pattern I_i . S_i is displaced outwards along the direction of the surface normals computed at each vertex v to create an outer finger surface S_i^O . Note, however, that the original electronic finger surface S_i is retained. The front portion S_i^{OF} and the rear portion S_i^{OR} of S_i^O are separated as only the front portion S_i^{OF} is used for projection.
3. **Preprocessing 2D calibration patterns:** If the pattern I_i being projected is a 2D fingerprint image, skeleton I_i^S of the image I_i is created. The ridge width of the skeleton I_i^S is increased using morphological operations, and the image is smoothed using a Gaussian filter before projecting it onto the frontal surface S_i^{OF} . This preprocessing step is important to ensure that ridges and valleys present in I_i are engraved smoothly onto S_i^{OF} . Note that preprocessing is not needed if any other 2D calibration pattern (e.g. sine grating) is being projected.
4. **Mapping 2D calibration patterns to 3D finger surfaces:** The front portion S_i^{OF} of the outer surface S_i^O is projected to 2D using the ISOMAP algorithm [TDSL00]. Rotation and flip are corrected using corresponding control points between front portion S_i^{OF} and the 2D projection of S_i^{OF} . Translation correction is done using the reference coordinates computed from I_i . The front portion S_i^{OF} is further subdivided depending on the resolution of I_i to ensure sufficient fidelity (high similarity scores for a FAR of 0.01%) of mapping I_i . Thereafter, the mapping between the vertex locations (x, y, z) on the front portion S_i^{OF} and the grayscale values at locations (u, v) in I_i is ascertained.
5. **Engraving 2D calibration patterns on 3D finger surfaces:** Ridges and valleys are engraved on S_i^{OF} by displacing the vertices on the front portion S_i^{OF} along the surface normals according to the texture values at the mapped (u, v) locations in I_i .
6. **Postprocessing 3D finger surfaces:** The front and rear portions of the outer finger surface S_i^O are combined. The original finger surface S_i is made as dense as the outer finger surface S_i^O and then the two surfaces are stitched together to create the 3D target A_i in electronic (virtual) form.
7. **Creating glove:** The middle portion M of the hand is displaced outward along the surface normals computed at each vertex v to create an outer replica M^O of M . M and M^O are then stitched together to create a wearable glove M^W . This finishes the creation of the six parts of the whole hand target in electronic form.
8. **3D Printing:** The thumb and four finger targets A_i and the glove M^W are physically fabricated using a 3D printer (Stratasys Objet350/500 Connex). Two different printing materials, TangoPlus FLX930 [Stb] and FLX9740-DM [Sta], are used to fabricate the thumb and four finger targets A_i as well as the glove M^W for contact-based slap fingerprint readers. These materials are semi-translucent whitish rubber-like materials with

Property	Human Skin [EM95] [FB93]	TangoPlus FLX930 [Stb]	FLX9740- DM [Sta]	RGD8520- DM [Sta]
Shore A hardness	20-41	26-28	35-40	N.A.
Tensile Strength (MPa)	5-30	0.8-1.5	1.3-1.8	40-60
Elongation at Break (%)	35-115	170-220	110-130	15-25

Tab. 1: Comparison of the mechanical properties of the three printing materials used for 3D whole hand target fabrication with the human skin. TangoPlus FLX930 and FLX9740-DM are rubber-like materials similar in mechanical properties to the human skin and are suitable for use with contact-based slap readers. RGD8520-DM is a rigid opaque material that provides optimum fingerprint ridge-valley contrast for use with the contactless slap reader.

similar hardness and elasticity as human skin (see Tab. 1). Unlike the black rubber-like materials used in our earlier work [Ar16], these materials are optically suitable for imaging with a variety of contact-based optical fingerprint readers. A bluish-gray rigid opaque material, RGD8520-DM [Sta], is used to manufacture the individual thumb and finger targets A_i for the contactless slap reader (see Tab. 1). This material provides optimum contrast between fingerprint ridges and valleys for imaging with the contactless slap reader. The wearable glove M^W for the contactless slap reader is fabricated with TangoPlus FLX930.

9. **Chemical Cleaning:** The majority of the printer support material is removed manually from the 3D printed parts. After this, the 3D printed parts are soaked in 2M NaOH solution for 3 hours, and then rinsed with water to remove the printer support material residue.
10. **Part Assembling:** The cleaned physical parts A_i ($i = 1 \dots 5$) and M^W are assembled together with superglue to generate a wearable whole hand target W .

3 Fidelity of 3D Whole Hand Target Generation

To ascertain the fidelity¹⁰ of the whole hand target creation process, we assess how well the features present in the 2D calibration patterns are replicated on the electronic 3D hand target after the 2D to 3D projection of the patterns, and on the physical 3D hand target post 3D printing and cleaning. We create a right hand target using five different rolled fingerprints from NIST SD4 [WW92]. Two samples of the whole hand target are fabricated with the two printing materials, TangoPlus FLX930 and FLX9740-DM. Five different slap impressions of the hand target are captured using three different *Appendix F* certified contact-based slap readers, SR1, SR2 and SR3¹¹ (see, e.g., Fig. 4). SR1 and SR3 are 500 ppi readers whereas SR2 is a 1000 ppi reader. Comparisons between (i) 2D fingerprints from NIST SD4 and the frontal images of corresponding fingerprints engraved on the electronic 3D hand target, (ii) frontal images of fingerprints engraved on the electronic 3D hand target to corresponding plain prints extracted from slap impressions of the physical 3D hand target, and (iii) the 2D fingerprints used to generate the hand target to corresponding plain prints extracted from slap impressions of the physical 3D hand target, are made to ascertain the fidelity of the 3D whole hand target generation process. Furthermore, plain prints extracted from five different slap impressions of the 3D hand target are compared with each other to determine the consistency between different impressions of the target (intra-impression variability). Verifinger 6.3 SDK [Ne] is used for conducting all comparison experiments. All slap impressions are upsampled by a factor of 1.2 using bicubic interpolation to account for reduction in ridge spacing due

¹⁰ *Fidelity* means the degree of exactness with which the 2D calibration patterns are reproduced on the electronic and physical 3D hand target.

¹¹ Vendor names are not provided to maintain their anonymity in this evaluation.



Fig. 4: Sample slap impression of the 3D whole hand target captured using a contact-based slap reader.

Fingerprint	S0005 (index)	S0043 (middle)	S0083 (ring)	S0096 (little)	S0044 (thumb)
score	203	150	399	183	249

Tab. 2: Similarity scores between frontal images (2D) of individual fingerprints engraved on the electronic 3D hand target captured in Meshlab and the corresponding 2D fingerprint images from NIST SD4 used for target generation. Verifinger 6.3 SDK was used for generating similarity scores. The threshold on scores @FAR = 0.01% is 33.

TangoPlus FLX930				FLX9740-DM			
Fingerprint	SR1 (500 ppi)	SR2 (1000 ppi)	SR3 (500 ppi)	Fingerprint	SR1 (500 ppi)	SR2 (1000 ppi)	SR3 (500 ppi)
S0005 (index)	87	68	168	S0005 (index)	147	159	78
S0043 (middle)	66	71	122	S0043 (middle)	48	201	107
S0083 (ring)	327	171	158	S0083 (ring)	362	441	222
S0096 (little)	173	141	108	S0096 (little)	140	156	129
S0044 (thumb)	65	69	93	S0044 (thumb)	63	62	50

Tab. 3: Similarity scores between the frontal images (2D) of the individual fingerprints engraved on the electronic 3D hand target and the corresponding plain prints extracted from a slap image of the physical 3D hand targets captured by each of the three contact-based slap readers (SR1, SR2 and SR3). Physical targets were fabricated with two different materials (TangoPlus FLX930 and FLX9740-DM). Verifinger 6.3 SDK was used for generating similarity scores. The threshold on scores @FAR = 0.01% is 33.

to 2D to 3D projection and 3D printing before conducting matching experiments (see [Ar16] for 2D to 3D projection and 3D printing fabrication error measurements).

3.1 Replication of 2D calibration pattern features on electronic 3D hand target

Frontal images of individual fingerprints engraved on the electronic 3D hand target are captured using Meshlab [Me]. They are rescaled manually to approximately the same scale as the 2D fingerprints from NIST SD4. Each individual fingerprint image from the electronic 3D target is compared to the corresponding 2D fingerprint from NIST SD4. Tab. 2 shows the similarity scores obtained for this experiment. All similarity scores are significantly above the verification threshold of 33 @FAR=0.01% for NIST SD4. This demonstrates that the features present in the 2D calibration patterns are replicated with high fidelity on the electronic 3D hand target.

TangoPlus FLX930				FLX9740-DM			
Fingerprint	SR1 (500 ppi)	SR2 (1000 ppi)	SR3 (500 ppi)	Fingerprint	SR1 (500 ppi)	SR2 (1000 ppi)	SR3 (500 ppi)
S0005 (index)	549	141	321	S0005 (index)	719	570	510
S0043 (middle)	213	161	315	S0043 (middle)	221	579	357
S0083 (ring)	441	374	411	S0083 (ring)	426	596	303
S0096 (little)	308	392	423	S0096 (little)	419	510	366
S0044 (thumb)	209	422	345	S0044 (thumb)	119	404	371

Tab. 4: Similarity scores between the plain prints extracted from slap impressions captured by the three contact-based readers (SR1, SR2 and SR3) of the physical 3D hand targets and the corresponding fingerprints from NIST SD4 used in their generation. Physical targets were fabricated with two different materials (TangoPlus FLX930 and FLX9740-DM). Verifinger 6.3 SDK was used for generating similarity scores. The threshold on scores @FAR = 0.01% is 33.

TangoPlus FLX930				FLX9740-DM			
Fingerprint	SR1 (500 ppi)	SR2 (1000 ppi)	SR3 (500 ppi)	Fingerprint	SR1 (500 ppi)	SR2 (1000 ppi)	SR3 (500 ppi)
S0005 (index)	839-1373	603-1193	797-1434	S0005 (index)	980-1359	735-1271	779-1229
S0043 (middle)	551-930	501-909	581-1206	S0043 (middle)	579-1079	855-1265	539-1190
S0083 (ring)	756-1127	843-1290	990-1272	S0083 (ring)	837-1254	924-1467	897-1503
S0096 (little)	644-1071	344-1133	957-1413	S0096 (little)	639-1043	710-1059	630-1221
S0044 (thumb)	800-1061	743-1263	989-1160	S0044 (thumb)	723-1178	845-1796	822-1469

Tab. 5: Range of similarity scores for pairwise comparisons between plain prints of the same finger extracted from five different slap prints captured by the three contact-based slap readers (SR1, SR2 and SR3) of the same 3D whole hand target. Results are shown for two physical hand targets fabricated with the two printing materials (TangoPlus FLX930 and FLX9740-DM). Verifinger 6.3 SDK was used for generating similarity scores. The threshold on scores @FAR = 0.01% is 33.

3.2 Replication of electronic 3D hand target features on physical 3D hand target

Individual plain prints are manually extracted (for convenience) from the slap impressions captured using the three contact-based slap readers. Each plain print is compared to the frontal image of the corresponding fingerprint engraved on the electronic 3D hand target. All similarity scores are well above the verification threshold of 33 @FAR=0.01% for NIST SD4 (see Tab. 3). This shows that features engraved on the electronic 3D target are preserved post 3D printing and cleaning.

3.3 Replication of 2D calibration pattern features on physical 3D hand target

Plain prints extracted from the slap impressions of the physical 3D hand target, captured using the three contact-based slap readers, are compared to corresponding 2D fingerprints from NIST SD4. Tab. 4 shows the similarity scores obtained for this experiment. Because all similarity scores are well above the verification threshold score of 33 @FAR=0.01% for NIST SD4, it can be inferred that the 2D calibration pattern features are replicated with high fidelity on the physical 3D hand target.

3.4 Consistency between different impressions of the physical 3D hand target

Individual plain prints extracted from different slap impressions of the same physical 3D hand target are compared with each other to measure their intra-class similarity. Similarity scores

TangoPlus FLX930			
Fingerprint	SR1 (500 ppi)	SR2 (1000 ppi)	SR3 (500 ppi)
index (7.82)	$\mu = 8.06, \sigma = 0.10$	$\mu = 7.87, \sigma = 0.06$	$\mu = 7.90, \sigma = 0.05$
middle (8.33)	$\mu = 8.64, \sigma = 0.03$	$\mu = 8.57, \sigma = 0.06$	$\mu = 8.35, \sigma = 0.08$
ring (8.62)	$\mu = 8.58, \sigma = 0.05$	$\mu = 8.65, \sigma = 0.10$	$\mu = 8.65, \sigma = 0.07$
little (8.47)	$\mu = 8.49, \sigma = 0.07$	$\mu = 8.49, \sigma = 0.10$	$\mu = 8.49, \sigma = 0.04$
thumb (7.67)	$\mu = 7.67, \sigma = 0.04$	$\mu = 7.66, \sigma = 0.06$	$\mu = 7.67, \sigma = 0.06$

FLX9740-DM			
Fingerprint	SR1 (500 ppi)	SR2 (1000 ppi)	SR3 (500 ppi)
index (7.82)	$\mu = 7.87, \sigma = 0.08$	$\mu = 7.80, \sigma = 0.08$	$\mu = 8.00, \sigma = 0.08$
middle (8.33)	$\mu = 8.61, \sigma = 0.09$	$\mu = 8.64, \sigma = 0.05$	$\mu = 8.36, \sigma = 0.05$
ring (8.62)	$\mu = 8.63, \sigma = 0.14$	$\mu = 8.66, \sigma = 0.03$	$\mu = 8.64, \sigma = 0.10$
little (8.47)	$\mu = 8.52, \sigma = 0.10$	$\mu = 8.51, \sigma = 0.14$	$\mu = 8.54, \sigma = 0.08$
thumb (7.67)	$\mu = 7.66, \sigma = 0.07$	$\mu = 7.66, \sigma = 0.03$	$\mu = 7.67, \sigma = 0.05$

Tab. 6: Mean (μ) and std. deviation (σ) of center-to-center ridge spacings (in pixels) in the plain prints extracted from five different slap images of the 3D whole hand targets captured using the three contact-based slap readers (SR1, SR2 and SR3). Expected average ridge spacing (in pixels) for each 2D fingerprint from NIST SD4 is shown in brackets. The spacing measurements take into consideration the reduction in spacing due to 2D to 3D projection and 3D printing fabrication errors.

for this experiment are reported in Tab. 5. All similarity scores are significantly above the verification threshold score of 33 @FAR=0.01% indicating that multiple slap impressions of the same 3D hand target are highly consistent.

4 Evaluating Contact-based Slap Fingerprint Readers

Center-to-center ridge spacing measurements are computed (using the method proposed in [HWJ98]) in the plain prints extracted from five different slap impressions captured using the three contact-based slap readers. We compare these measurements against the expected average center-to-center ridge spacing in the corresponding 2D fingerprints used during target creation. The expected ridge spacing is computed taking into consideration the 2D to 3D projection error (5.8%) and the 3D printing fabrication error (11.42%) that were estimated in our earlier work [Ar16]. Tab. 6 lists the measurements taken from slap impressions of the two hand targets. Following are some observations based on this experiment:

- The estimated ridge spacings in slap impressions of the hand targets captured using the three contact-based slap readers, SR1, SR2 and SR3 are, on average, within 0.08 pixels of each other. In other words, all three slap readers SR1, SR2 and SR3 perform equally well in preserving fingerprint ridge spacing.
- The estimated ridge spacings in the plain prints of index, middle, ring and little fingers are, on average, marginally greater than the expected ridge spacing. Although the increase in ridge spacings is not as significant as that reported in our earlier work *et al.* [Ar16] for single-finger 3D targets, it is consistent with our observation. This increase in ridge spacing is due to the flattening of the finger skin because of the pressure applied on the reader platen while capturing fingerprints. For the thumb, however, this flattening effect is not observed to be as profound compared to the other fingers, and does not seem to impact the ridge spacing measurements. One possible reason could be the difference in pressure on the reader platen for each finger while capturing slap impressions. A better understanding of the underlying cause would require controlled

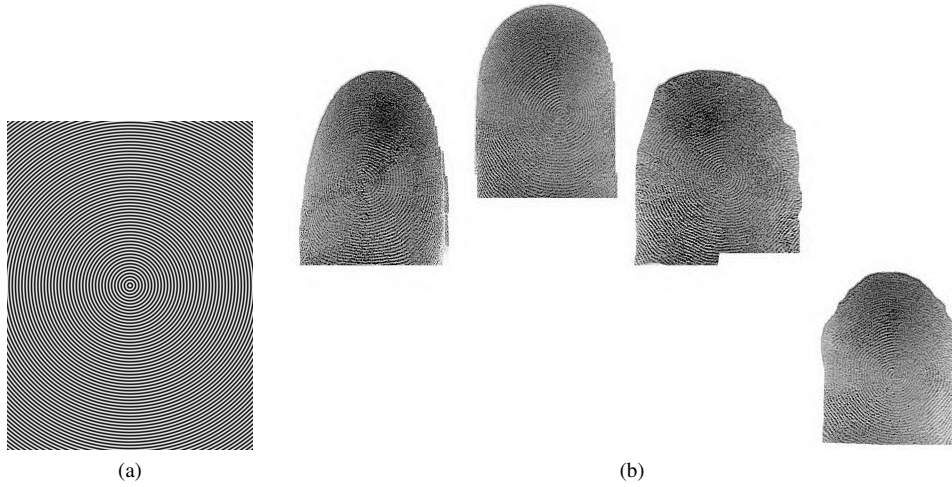


Fig. 5: Circular sine grating (ridge spacing = 10 pixels) used to generate the 3D whole hand target (shown in (a)) and the slap impression of the corresponding hand target captured using the contactless slap reader (shown in (b)).

experimentation where known contact pressure is applied by each finger during fingerprint capture. This is a topic of future research.

- Fabrication material of the hand target does not seem to significantly impact the ridge spacing measurements in fingerprint images captured using the three slap readers.

5 Evaluating Contactless Slap Fingerprint Reader

The contactless slap reader used in our experiment is a *PIV* certified 500 ppi reader that captures a 512×512 image of each fingertip from a single wave of the hand. Therefore, for evaluating the contactless slap reader, we generated a right whole hand target by projecting circular sine gratings of fixed ridge spacing (10 pixels) such that they cover the entire fingertip¹². The rigid opaque material RGD8520-DM was used to fabricate the thumb and four finger targets whereas rubber-like flexible material TangoPlus FLX930 was used to manufacture the fingerless glove so that it is easy to wear. Five different slap impressions of the whole hand target were captured using the contactless slap reader (see, e.g., Fig. 5). Analogous to the earlier experiment, center-to-center ridge spacing measurements are computed in the plain prints extracted from five different slap impressions captured using the contactless slap reader. We compare these measurements against the expected average center-to-center ridge spacing in the circular gratings used during target creation. The expected ridge spacing takes into consideration the 2D to 3D projection error (5.8%) and the 3D printing fabrication error (11.42%) [Ar16]. Tab. 7 lists the measurements taken from contactless slap impressions of the hand target. Following are some observations based on this experiment:

- The average deviation in estimated center-to-center ridge spacings in slap impressions of the circular grating hand target is about 0.25 pixels from the expected ridge spacing. Further analysis is needed to interpret this measurement and understand, in more details, the effects of the unconstrained nature of contactless fingerprint capture, the size of the captured area as well as the nature of the material used to create the target.

¹² We are designing a method to do a similar projection for fingerprints.

RGD8520-DM	
Fingerprint	CR (500 ppi)
index	$\mu = 8.12, \sigma = 0.16$
middle	$\mu = 8.35, \sigma = 0.10$
ring	$\mu = 8.28, \sigma = 0.15$
little	$\mu = 8.03, \sigma = 0.15$
thumb	$\mu = 7.67, \sigma = 0.08$

Tab. 7: Mean (μ) and std. deviation (σ) of center-to-center ridge spacings (in pixels) in the plain prints extracted from five different slap images of the circular grating whole hand target captured using the contactless slap fingerprint reader (CR). Expected average ridge spacing (in pixels) of the circular grating engraved on the hand target is 8.28. The spacing measurements take into consideration the reduction in spacing due to 2D to 3D projection and 3D printing fabrication errors.

- The estimated ridge spacings in the plain prints of index, middle, ring and little fingers are, on average, closer to the expected ridge spacing compared to the thumb. This may be because the four fingers are captured together in a slap impression whereas thumb is captured individually as a separate impression, and the user dynamics involved in the two capture processes (e.g. finger alignment with respect to the optical capture, relative finger movement) are quite different. Controlled experimentation where the relative positioning of the user’s fingers/hand with respect to the reader is fixed at the time of contactless slap capture is required to investigate this further. It is a topic of future research.

6 Conclusions and Ongoing Work

We have presented a method to design and fabricate whole hand 3D targets for evaluating multi-finger capture devices, e.g., contact-based and contactless slap fingerprint readers. 2D calibration patterns of known characteristics (e.g. fingerprints of known ridge flow and ridge spacing, sine gratings of known orientation and center-to-center spacing) are projected onto a generic 3D hand model to create an electronic 3D hand target. Physical 3D hand target is fabricated from the electronic target using a state-of-the-art 3D printer. Material(s) similar in hardness and elasticity to the human skin as well as optically suitable for use with a variety of fingerprint readers are used for 3D hand target fabrication. Our experimental results show that features present in the 2D calibration patterns are replicated with high fidelity both on the electronic and physical 3D hand target during the 3D hand target generation process. We also conduct experiments to evaluate three *Appendix F* certified slap readers and a *PIV* certified contactless slap reader using the fabricated 3D hand targets. To the best of our knowledge, this is the first study that demonstrates the utility of the 3D wearable hand targets for evaluation of slap readers, both contact and contactless.

Given that state-of-the-art high-resolution 3D printers cannot fabricate 3D hand targets with rubber-like conductive materials, we are investigating methods to impart conductivity to the 3D printed hand targets. This would enable evaluation of capacitive fingerprint readers using these targets. We also plan to study how user-induced variabilities, e.g. contact-force applied on the reader platen and relative finger orientations with respect to each other as well as the reader platen, impact the quality of the captured fingerprint images.

Acknowledgements

This research was supported by grant no. 60NANB11D155 from the NIST Measurement Science program. The authors would like to thank Matthew Staymates, National Institute of

Standards and Technology, and Brian Wright, Michigan State University for their help with 3D printing of the whole hand targets. They would also like to acknowledge 3M Cogent, Crossmatch, Morpho and Suprema for their assistance in this study.

References

- [Aa] Aadhaar, Unique Identification Authority of India, <http://uidai.gov.in/>.
- [Ar16] Arora, S. S.; Cao, K.; Jain, A. K.; Paulter Jr, N. G.: Design and Fabrication of 3D Fingerprint Targets. *IEEE Transactions on Information Forensics and Security*, 11(10):2284–2297, 2016.
- [Co] Contactless Fingerprint Capture, National Institute of Standards and Technology, http://www.nist.gov/itl/iad/ig/contactless_fingerprint.cfm.
- [EM95] Edwards, C.; Marks, R.: Evaluation of biomechanical properties of human skin. *Clinics in Dermatology*, 13(4):375–380, 1995.
- [Fa] Faster and Better Fingerprinting: The Fast Capture Initiative, National Institute of Justice, <http://www.nij.gov/topics/technology/biometrics/pages/fast-capture-initiative.aspx>.
- [FB] FBI IAFIS certified product listing, http://www.fbi.gov/about-us/cjis/fingerprints_biometrics/iafis/iafis_cert.
- [FB93] Falanga, V.; Bucalo, B.: Use of a durometer to assess skin hardness. *Journal of the American Academy of Dermatology*, 29(1):47–51, 1993.
- [HWJ98] Hong, L.; Wan, Y.; Jain, A. K.: Fingerprint image enhancement: algorithm and performance evaluation. *IEEE Transactions on Pattern Analysis and Machine Intelligence*, 20(8):777–789, 1998.
- [Lo87] Loop, C.: Smooth subdivision surfaces based on triangles. Master’s thesis, University of Utah, 1987.
- [Me] Meshlab, <http://sourceforge.net/projects/meshlab/>.
- [Ne] NeuroTechnology Verifinger SDK 6.3, <http://www.neurotechnology.com/verifinger.html>.
- [Ne12] Next Generation Identification, Federal Bureau of Investigation, http://www.fbi.gov/about-us/cjis/fingerprints_biometrics/ngi.
- [Ni06] Nill, N. B.: Test procedures for verifying image quality requirements for personal identity verification (PIV) single finger capture devices. Technical Report MTR 060170, MITRE, 2006.
- [Ni13] Nill, N. B.: Test procedures for verifying IAFIS image quality requirements for fingerprint scanners and printers V 1.4. Technical Report MTR 05B0016R7, MITRE, 2013.
- [Of] Office of Biometric Identity Management Identification Services, <http://www.dhs.gov/obim-biometric-identification-services>.
- [PC06] Peyré, G.; Cohen, L. D.: Geodesic remeshing using front propagation. *International Journal of Computer Vision*, 69(1):145–156, 2006.
- [PC09] Parziale, G.; Chen, Y.: Advanced Technologies for Touchless Fingerprint Recognition. In (Tistarelli, M.; Li, S. Z.; Chellappa, R., eds): *Handbook of Remote Biometrics, Advances in Pattern Recognition*, pp. 83–109. Springer, 2009.
- [Re] Recording Legible Fingerprints, Federal Bureau of Investigation, https://www.fbi.gov/about-us/cjis/fingerprints_biometrics/recording-legible-fingerprints.
- [Sta] Stratasys Digital Materials Data Sheet, http://usglobalimages.stratasys.com/Main/Files/Material_Spec_Sheets/MSS_PJ_DigitalMaterials_Datasheet.pdf?v=635832868828035876.
- [Stb] Stratasys PolyJet Materials Data Sheet, http://usglobalimages.stratasys.com/Main/Files/Material_Spec_Sheets/MSS_PJ_PJMaterialsDataSheet.pdf?v=635785205440671440.
- [TDSL00] Tenenbaum, J. B.; De Silva, V.; Langford, J. C.: A global geometric framework for nonlinear dimensionality reduction. *Science*, 290(5500):2319–2323, 2000.
- [WW92] Watson, C. I.; Wilson, C. L.: NIST Special Database 4. Fingerprint Database, National Institute of Standards and Technology, 17:77, 1992.